Since January 2020 Elsevier has created a COVID-19 resource centre with free information in English and Mandarin on the novel coronavirus COVID-19. The COVID-19 resource centre is hosted on Elsevier Connect, the company's public news and information website.

Human Pathology (2006) 37, 381–390

ELSEVIER

Human PATHOLOGY

www.elsevier.com/locate/humpath

Perspectives in pathology

The comparative pathology of severe acute respiratory syndrome and avian influenza A subtype H5N1—a review

Wai-Fu Ng MBBS, FRCPath[a,*], Ka-Fai To MBBS, FRCPath[b], William W.L. Lam MBBS, FHKAM(Path)[a], Tak-Keung Ng MBBS, FRCPath[a], Kam-Cheong Lee MBBS, FRCPath[a]

[a]*Department of Pathology, Princess Margaret Hospital, Kowloon West Cluster Hospitals, Hong Kong Special Administrative Region, China*
[b]*Department of Anatomical and Cellular Pathology, the Chinese University of Hong Kong, Prince of Wales Hospital, Shatin, New Territories, Hong Kong Special Administrative Region, China*

Received 11 November 2005; revised 6 January 2006; accepted 12 January 2006

Keywords:
Severe acute respiratory syndrome;
SARS;
Avian influenza;
H5N1;
Diffuse alveolar damage;
Pathology

Summary The pathology of 2 zoonotic human viral infections that recently emerged, severe acute respiratory syndrome (SARS) due to coronavirus (SARS-CoV) and avian influenza A subtype H5N1, is reviewed and compared based on the literature and the cases examined by the authors. Pneumocytes are the primary target of infection resulting in diffuse alveolar damage. Systemic cytokine activation results in hemophagocytic syndrome, lymphoid depletion, and skeletal muscle fiber necrosis. Severe acute respiratory syndrome induces a more fibrocellular intra-alveolar organization with a "bronchiolitis obliterans organizing pneumonia"–like pattern and presence of multinucleated histiocytes and pneumocytes. H5N1 causes a more fulminant and necrotizing diffuse alveolar damage with patchy and interstitial paucicellular fibrosis. Severe acute respiratory syndrome associated coronavirus persists in the lung up to the second month, whereas H5N1 persists in the lung up to the third week. Severe acute respiratory syndrome associated coronavirus disseminates to blood, urine, feces, gastrointestinal tract, and liver. There is recent report of possible cerebral involvement by H5N1 and its isolation in the blood, gastrointestinal tract, and cerebrospinal fluid. More pathologic studies are urgently needed.

1. Introduction

Severe acute respiratory syndrome (SARS) due to coronavirus (SARS-CoV) was retrospectively first recognized in Guangdong, the southern province of China, in November 2002 [1]. Spreading through travelers, major outbreaks occurred in China, Hong Kong, Vietnam, Singapore, and Canada in 2003. Globally, 8422 people were infected with 916 deaths and a case fatality ratio of 11% [2]. After successful termination of the outbreak in July 2003, sporadic zoonotic or laboratory-acquired cases had occurred. The natural reservoir of SARS-CoV has not been identified, but a number of wildlife species, including the

* Corresponding author. Department of Pathology, Yan Chai Hospital, Tsuen Wan, NT, Hong Kong.
E-mail address: ngwaifu@cuhk.edu.hk (W.-F. Ng).

0046-8177/$ – see front matter © 2006 Elsevier Inc. All rights reserved.
doi:10.1016/j.humpath.2006.01.015

masked palm civet, have shown laboratory evidence of infection with a related coronavirus [1]. The first documented human outbreak of avian influenza occurred in Hong Kong in 1997, with 18 persons infected and 6 deaths [3]. The etiologic agent was a highly pathogenic avian influenza A subtype H5N1. Human diseases were reported again from Hong Kong in 2003 [4]. From late 2003, human diseases became persistent in Southeast Asia. As of December 30, 2005, a total of 142 cases with 74 deaths were reported, and the case fatality ratio was 52% [5]. The countries with confirmed cases include Cambodia, Thailand, Vietnam, Indonesia, and China. From late 2005, animal cases of H5N1 were also reported from Russia, Romania, Turkey, and other European countries. At the time of writing this article, the first documented human case outside Asia was reported in Turkey. The strains of the H5N1 in these outbreaks may not be identical, but they are all highly pathogenic. Both SARS and avian influenza cause severe respiratory tract infection. Their rapid and definitive diagnosis is required both for proper management of the patients and for public health implication. The purpose of this study is to review and compare the anatomical pathology of SARS and H5N1 based on the published literature. The findings on a few cases of SARS and H5N1 examined by the authors were incorporated in this report and used in the illustration figures.

2. Materials and methods

A thorough search of the Medline database was performed on published reports on the human pathology of SARS and avian influenza A subtype H5N1. The terms used in the search were combination of *severe acute respiratory syndrome* or *avian influenza* (as subject heading) and *pathology* (as keyword but not subject heading). Original pathology reports were the primary target of this review, but clinical reports with pathology findings were also included if contributory. All the English full-text reports were retrieved and reviewed. A few original pathology reports in Chinese were excluded. The pathology of the 2 diseases was separately summarized and then compared. The pathology material on 2 postmortem cases of SARS, 1 liver biopsy from a patient with SARS, and 2 full postmortem cases of H5N1 examined by the authors were incorporated in this review and used in the figures, which are newly taken photomicrographs. These cases have all been previously reported. The pathology material used in the illustration was from standard paraffin blocks processed for hematoxylin and eosin sections. For immunohistochemistry, paraffin-embedded sections were used. The antigen retrieval process was done by wet heating of sections in a pressure cooker. The primary antibodies used were from mouse and the secondary antibody was from rabbit. The reaction was detected by a peroxidase method using the DAKO detection kit on DAKO Cytomation (Glostrup, Denmark). The manufacturer and dilution of the antibodies used were as follows: CD3, DAKO, 1:150; CD20, DAKO, 1:750; CD30, DAKO, 1:5; CD56, ZYMED, 1:250; CD68, DAKOPATTS, 1:2500; AE1/AE3, DAKO, 1:30.

3. Results

3.1. Review of the pathology of SARS

Pathology of SARS, mainly of the pulmonary system, was reported from Hong Kong by Nicholls et al [6], Tse et al [7], and Cheung et al [8]; from mainland China by Lang et al [9] and Ding et al [10]; from Taiwan by Hsiao et al [11]; from Singapore by Franks [12] and Chong et al [13]; and from Canada by Hwang et al [14]. There were a few reports on other specific organ systems affected by SARS-CoV including liver [15], gastrointestinal tract [16], skeletal muscle [17], kidney [18] and hematolymphoid organs [19]. The major findings of these series are summarized in Table 1. There were also a number of reports on the immunohistochemical, in situ hybridization, and ultrastructural localization of SARS-CoV in pathologic specimens [20-22]. The 2 SARS cases used in the illustration were reported in a clinical article [23] and as one of the cases of reference [6]. In total, the pulmonary and general pathologic review of SARS included 62 patients based on the first 8 series in Table 1 plus author's cases. Apart from lung biopsies from 4 live patients, all materials were from postmortem cases. There were 38 men and 24 women with an average age of 59.6 years (range, 25-99 years). The age groupings by 10s were 2 for twenties, 8 for thirties, 8 for forties, 7 for fifties, 12 for sixties, and 16 for those 70 years or older (n = 53, excluding 9 with age not mentioned). The average duration from symptom onset to death was 19.5 days (median, 16 days; range, 4-108 days; n = 62). The distribution of death by weeks of disease duration was 6 for week 1, 16 for week 2, 20 for week 3, 7 for week 4, and 6 for week 5 or longer (n = 55).

Only a few reports recorded the amount of pleural effusion and the gross lung weight [6,7,13]. Straw color or hemorrhagic pleural effusion from 50 to 400 mL in each pleural cavity was noted. Gross lung weight of more than 1000 g on each side was commonly recorded with the highest documented weight of 2100 g [6]. However, lung weight down to 600 to 650 g on each side was also recorded. A lower lung weight occurred more commonly in patients dying in the first week or from coexisting diseases. The lungs grossly showed varying degree of congestion, edema, and consolidation. The pulmonary pathology reported was diffuse alveolar damage with varied terminology used, including acute or exudative phase, proliferative, or organizing phase and fibrotic phase. In general, patients in the initial 10 days of illness showed diffuse alveolar damage (DAD) in the acute or exudative phase including hyaline membrane formation (Fig. 1A). The

Table 1 Summary of major pathologic reports on SARS

Serial no.	First author/countries	No. of patients	Organs reported	Major pathologic findings	Reference
1	Nicholls/HK, China	6	Mainly lung	DAD (Fig. 1A-D), giant cells, enlarged pneumocytes, prominent macrophages (Fig. 1C and 1E1), white pulp atrophy of spleen (Fig. 2C), hemophagocytosis (Fig. 2A and B).	[6]
2	Tse/HK, China	7	Lung	DAD, multinucleated pneumocytes, BOOP-like pattern of organization (Fig. 1C and D).	[7]
3	Cheung/HK, China	10	Lung	DAD with organization and fibrosis, no specific histology	[8]
4	Lang/China	3	General autopsy	DAD, hemorrhagic necrosis in lymph node and spleen, lymphocyte depletion in spleen	[9]
5	Ding/China	3	General autopsy	DAD, necrosis in splenic lymphoid tissue and lymph node, systemic vasculitis	[10]
6	Hsiao/Taiwan, China	4	Lung	DAD, no specific histology, DAD absent in early stage	[11]
7	Franks/Singapore Chongs/ Singapore	8	Lung	DAD, acute phase in ≤10 days, organizing phase in >10 days, multinucleated pneumocyte and macrophages	[12,13]
8	Hwang/Canada	20	Lung	DAD in 8, acute fibrinous and organizing pneumonia in 6, mixed pattern in 6, multinucleated giant cells, fibrin thrombi	[14]
9	Chau/HK, China	3	Liver	accumulation of mitosis and apoptosis, ballooning hepatocytes, lobular inflammation (Fig. 2F).	[15]
10	Leung/HK, China	6	Intestinal tract	Minimal architectural disruption but with active viral replication in small and large intestine	[16]
11	Leung/HK, China	8	Skeletal muscle	Spectrum of myopathic changes, focal fiber necrosis common (Fig. 2D).	[17]
12	Chu/HK, China	7	Kidney	Acute tubular necrosis (Fig. 2E), normal glomeruli	[18]
13	Wong/HK, China	4	Hematolymphoid	Atrophic white pulp in spleen, active bone marrow, reactive hemophagocytosis not seen	[19]

NOTE. Figs. 1 and 2 are new photomicrographs showing pathologic changes in patients with SARS examined by the authors. Abbreviation: HK, Hong Kong.

major inflammatory cells in the alveoli were variably described as mixed inflammatory (Fig. 1B) or predominantly histiocytic. The earliest pulmonary findings were reported by Franks et al [12] on 2 patients at days 4 and 6 of illness with focal (<50%) and diffuse (>50%) acute DAD, respectively. Several authors had emphasized the focal nature of DAD in the initial 10 days and the diagnostic uncertainty especially on a biopsy specimen [6,8,11,13]. Proliferative or organizing changes with progression to fibrosis were noted in patients beyond day 10 (Fig. 1C and D). Even in these patients, the DAD could be patchy, but with a tendency for more diffuse involvement. Features of organizing DAD commonly coexisted with acute DAD in different parts of the lung (Fig. 1A, C, and D). Cheung examined 3 patients from day 29 to 46 and noted organizing and fibrotic DAD. Acute DAD was no longer seen except for a few remnant hyaline membranes [8]. The term *bronchiolitis obliterans organizing pneumonia (BOOP)–like pattern* was used by 3 authors including ourselves and 7 of the 14 studied cases showed such pattern (Fig. 1D) [6,7]. Hwang et al [14] reported the acute fibrinous and organizing pneumonia pattern as predominating in 6 of his 20 cases and in patients after day 20 of illness. This pattern of intra-alveolar fibrin balls and organizing pneumonia was first described by Beasley et al [24] as distinct from DAD and BOOP. The significance of this pattern is uncertain as it may be a variant of DAD. The lack of description of this pattern by other authors of SARS series may be because of inclusion of this pattern as a variant of DAD. Review of the 2 cases examined by the authors showed the coexistence of this pattern with other features of organizing DAD in one case. Multinucleated pneumocytes (Fig. 1E1) and histiocytes (Fig. 1E2) were documented in about 66%, but these could be absent or scanty. Atypical and enlarged pneumocytes with multinucleation, prominent nucleoli, chromatin clearing, and ample amphophilic granular cytoplasm had been well described by several authors [6,7,10,12]. These cells were suspected to harbor the SARS-CoV. However, viral inclusion was not evident. Regenerative hyperplasia of type 2 pneumocytes was prominent from the organizing phase (Fig. 1F). Other pathologic features included squamous metaplasia of respiratory epithelium, fibrin thrombi in pulmonary vessels, and focal honeycomb fibrosis. Complicating bronchopneumonia was noted in 13 patients (~21%),

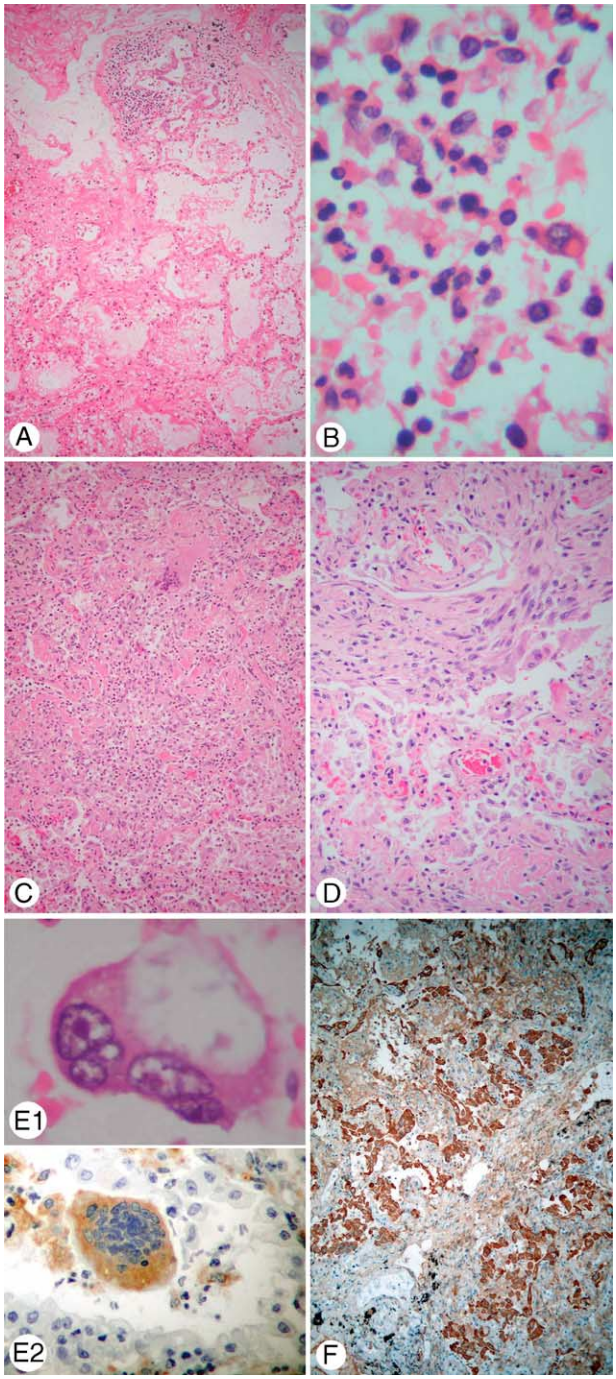

Fig. 1 Pulmonary pathology of SARS. A, Acute exudative DAD with hyaline membrane. B, Mixed inflammatory cells exudative in acute DAD. C, Organizing DAD with intra-alveolar fibrocellular infiltrate. Note a histiocytic giant cell in upper part of the field. D, BOOP-like pattern of organization. E1, Multinucleated pneumocyte. E2, Multinucleated histiocyte labeled with the histiocytic marker CD68. F, Pneumocytic regeneration labeled by the epithelial marker AE1/AE3 (hematoxylin-eosin stain unless specified, original magnification ×630 [B], ×1000 [E1], ×400 [E2], and ×100 [all others]; E1 taken from a patient with SARS dying on day 18, all others taken from a patient with SARS dying on day 20).

and superinfection by bacteria, fungus, and CMV was noted. The authors studied the immunoprofiles of the lymphoid cells in the lungs on 2 cases. In one patient who had not been given high-dose corticosteroid, the lymphoid cells were more abundant including both CD3-reactive T cells and CD20-reactive B cells. CD8-reactive T suppressor-cytotoxic cells appeared more than CD4-reactive T helper-inducer cells. CD30-reactive activated lymphoid cells were rare and CD56-reactive natural killer cells were absent. For the other patient treated with high-dose corticosteroid, the inflammatory infiltrate was significantly less but the cell types were similar.

Reverse transcriptase–polymerase chain reaction (RT-PCR) of lung tissue was positive for SARS-CoV on 43 of 49 cases. Electron microscopy (EM) for coronavirus on the lungs was positive on 12 of 14 cases. For the 6 cases with negative RT-PCR, EM was done in 5 and identified coronavirus in 3 of them. The longest duration of illness with a positive PCR result was day 42 (case 4 of the series by Cheung et al [8]). The longest duration with a positive EM result was day 46 (case 7 of Cheung's series). The longest duration of illness studied was day 108 (case 20 of the series by Hwang et al [14]) with negative PCR result but EM was not done. Twelve cases had both PCR and EM done. Seven cases were positive by both methods. One case was negative by both methods (day 16 of illness, case 5 of the series by Tse et al [7]). Four cases were PCR negative but EM positive. A PCR-positive and EM-negative case was not found.

There were only a few reports on the extrapulmonary pathology of SARS (series 9 to 13 of Table 1). In the 2 cases studied by the authors, hemophagocytic syndrome in the pulmonary hilar lymph nodes and bone marrow were noted (Fig. 2A and B). The study by Wong et al [19] on 4 autopsied cases showed no hemophagocytic syndrome. Lymphoid depletion in the spleen (Fig. 2C) and lymph node were noted by several authors [6,10,11,14,19]. Focal necrosis or apoptosis in lymph nodes and spleen was reported by Lang et al [9] and Ding et al [10]. Although diarrhea and fecal excretion of SARS-CoV were common, biopsied or autopsied material showed no pathologic changes in the gastrointestinal tract. However, active viral replication in both small and large intestinal enterocytes was demonstrated [16]. Chau et al [15] reported SARS-CoV–associated hepatitis in 3 patients with accumulation of mitosis and apoptosis (Fig. 2F) and positive RT-PCR result on the liver tissue. Such hepatitis was not observed in the autopsied series. Leung et al [17] reported myopathic changes (Fig. 2D) associated with SARS in a postmortem series of 8 cases. However, direct invasion of skeletal muscle by SARS-CoV was not evident. Acute tubular necrosis of the kidneys (Fig. 2E) was reported by several authors [10,13,18]. Systemic vasculitis was described by Ding, but the illustration showed leukocytes margination and stasis with no definite destruction of vascular wall. Vasculitis was not reported by the other authors. No specific changes were noted in the other organs.

Macrovesicular steatosis and centrilobular necrosis of liver, ischemic necrosis of heart, and adrenal hemorrhage were considered nonspecific features related to hypoxemia and shock. Myocarditis was not seen. The brains of the 2 cases studied by the authors showed no encephalitis or specific changes. In one of our cases, RT-PCR, viral culture, and EM of the kidney were positive for SARS-CoV, but RT-PCR of the liver and bone marrow was negative. By in situ hybridization and other techniques, SARS-CoV was localized to pneumocytes, macrophages, and enterocytes [20,21]. Ding et al [22] reported a more broad distribution in other organs but was not confirmed by others. In a clinical article, positive RT-PCR for SARS-CoV was reported from the cerebrospinal fluid of a patient with SARS after a generalized tonic-clonic convulsion, whereas the RT-PCR for SARS-CoV of the concurrent serum was negative [25].

3.2. Review of the pathology of avian influenza A H5N1

There were very few reports on the pathology of H5N1 infection. Three autopsied cases were reported from Hong Kong [4,26]. For the outbreak in Southeast Asia, pathologic findings were reported on 5 fatal cases from Thailand [27-30]. Thus, this review consisted of only 8 patients, which are summarized in Table 2. The pathologic material used in the illustration was from cases 1 and 3, which were examined by the authors. Thus, there is a severe limitation on the pathologic data available for H5N1. The gross pulmonary findings showed extensive consolidation with varying degree of hemorrhage. In a fatal case on day 10 (case 3), the lungs were reddish brown, solid, and weighed more than 1000 g (right, 1170 g; left, 1020 g). There was also bilateral lightly blood-stained effusion (right, 700 mL; left, 900 mL). The pulmonary pathology was diffuse alveolar damage plus interstitial lymphoplasmacytic infiltration and fibrosis. The DAD was in the acute exudative phase (Fig. 3A and B) for patients dying in the first 2 weeks and was in organizing phase (Fig. 3D and E) for patients dying in the third week or later. In the acute phase, the major cell types in the alveoli were macrophages, neutrophil, and activated lymphocyte (Fig. 3C). Necrotizing alveoli were noted in the acute phase (Fig. 3B), and the destruction of alveoli explained the patchy fibrosis without regenerating pneumocytes (Fig. 3D and F). There was also interstitial fibrosis. The fibrosis appeared hyaline and paucicellular. Specifically, intra-alveolar fibrosis with a BOOP-like pattern was not observed, in contrast to that of SARS (Fig. 1C, D, and F). Reactive hyperplasia of pneumocytes was present in the organizing phase (Fig. 3F) and viral inclusion was absent. Multinucleated cells were not described. Bronchiolitis with squamous metaplasia was seen. Honeycomb dilatation was noted in a patient dying at 1 month (case 1). Superinfection by *aspergillosis* was noted in 1 patient (case 5). The authors studied the immunophenotypes of the lymphoid cells in the lungs of case 3. CD3-reactive T cells

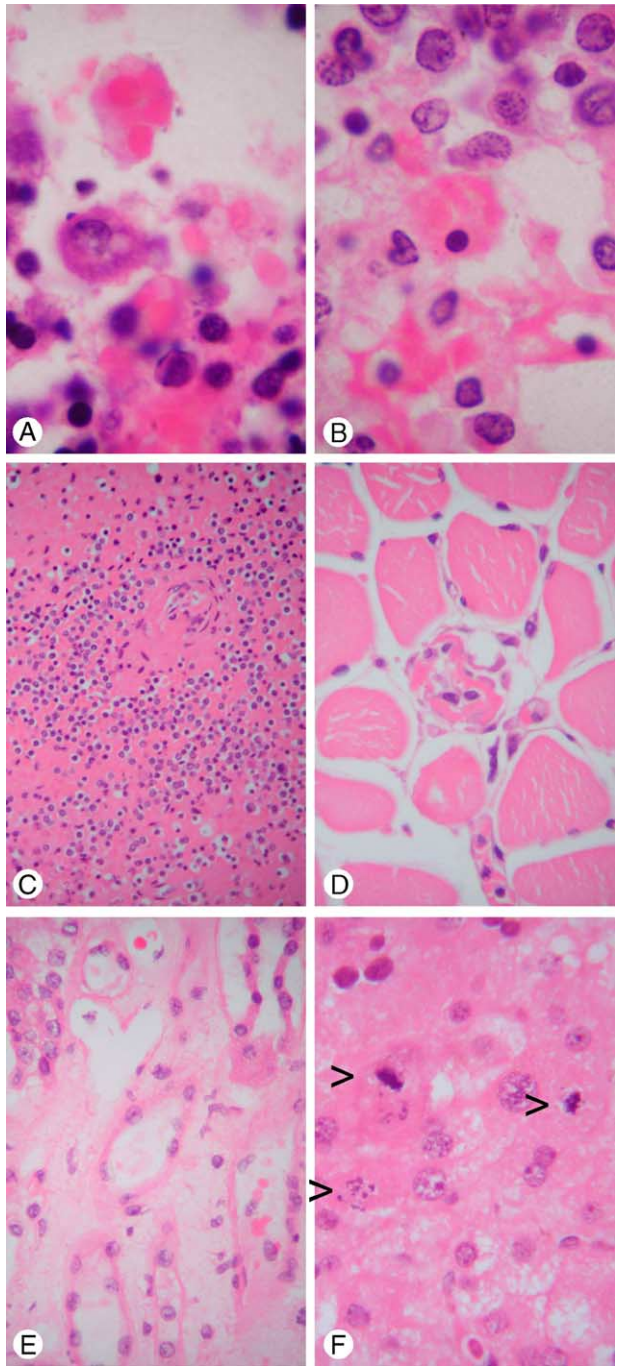

Fig. 2 Extrapulmonary pathology of SARS. A, Reactive hemophagocytosis in pulmonary hilar lymph node. B, Reactive hemophagocytosis in bone marrow. C, Lymphoid depletion in spleen. D, Skeletal muscle fiber necrosis. E, Acute tubular necrosis of kidney compared with normal tubule at left upper corner. F, Mitosis and apoptosis of hepatocytes (arrowheads) and ballooning degeneration in SARS-CoV–associated hepatitis (hematoxylin-eosin stain, original magnification ×1000 [A and B] and ×400 [all others]; A and B taken from a patient with SARS dying on day 18; C-E taken from a patient with SARS dying on day 20; F taken from liver biopsy of a patient with SARS on day 31).

Table 2 Summary of pathologic reports on H5N1

Case	Sex/age	Year/countries	Duration of disease (d)	Major pathologic findings	Reference
1	F/13	1997/ Hong Kong	30	Organizing DAD with interstitial fibrosis (Fig. 3D-F), reactive hemophagocytic syndrome, lymphoid depletion (Fig. 4C), hepatic centrilobular necrosis, acute renal tubular necrosis, microglial nodules with demyelination in cerebral white matter (Fig. 4E and F).	[26]
2	F/25	1997/ Hong Kong	30	Similar to above except for normal brain, presence of extramedullary hematopoiesis and focal necrosis in lymph node	[26]
3	M/33	2003/ Hong Kong	10	Acute DAD (Fig. 3A-C), reactive hemophagocytic syndrome (Fig. 4A and B), activated lymphoid cells in reticuloendothelial system, lymphoid depletion, skeletal muscle fiber necrosis (Fig. 4D), acute renal tubular necrosis, normal brain	[4]
4	F/26	2004/ Thailand	10	DAD, interstitial pneumonia, cholestasis, hemophagocytic activity in liver, lymphoid depletion in spleen	[27]
5	M/6	2004/ Thailand	17	Consolidated lungs with focal hemorrhage, DAD, interstitial lymphoplasmacytic infiltrate, bronchiolitis, histiocytosis in lymphoid system but no hemophagocytosis, reactive hepatitis, small foci of necrosis in brain	[28,29]
6, 7, 8	Not specified	2004/ Thailand	Not specified	Lung and spleen examined only, DAD with hyaline membrane, reactive fibroblasts and hemorrhage, atypical lymphocytes in spleen.	[30]

NOTE. Figs. 3 and 4 are new photomicrographs showing pathologic changes in case 1 and 3 examined by the authors.

were more numerous than CD20-reactive B cells. CD4-reactive T helper-inducer cells appeared more than CD8-reactive T suppressor-cytotoxic cells. Some of the larger activated lymphoid cells were reactive with the activation marker CD30. These cells were also observed in the lymphoreticular system including the spleen (Fig. 4C), tonsil, and lymph node. In the lung, CD56-reactive natural killer cells were rare.

The lymphoreticular system was marked by histiocytic hyperplasia. Reactive hemophagocytic syndrome was noted in 4 cases (cases 1-4) (Fig. 4A and B). Large activated lymphoid cells were present in the lymphoreticular system (Fig. 4A and C inset). The spleen showed atrophic white pulp and congested red pulp (Fig. 4C). The bone marrow varied from hypocellular (case 1) to hypercellular (cases 2 and 3). Extramedullary hemopoiesis was noted in the lymph node, spleen, and liver in 1 patient dying at 1 month (case 2). The liver showed mild macrovesicular steatosis. In 2 cases, centrilobular necrosis was noted (cases 1 and 2). Kupffer cell hyperplasia with occasional hemophagocytosis was also noted. Widespread microvesicular steatosis of Reye's syndrome was not observed. Acute tubular necrosis was noted in 3 cases (cases 1-3). Skeletal muscle fiber necrosis was documented in 2 cases (cases 1 and 3) (Fig. 4D). In the 13-year-old girl dying at 1 month (case 1), the cerebral white matter showed scattered microglial nodules with hemorrhage, rarefaction, demyelination, axon balls, and foamy or pigment-laden macrophages (Fig. 4E and F). However, no perivascular lymphocytic cuffing or ventriculitis was observed. Small foci of necrosis in the brain were also reported in the 6-year-old boy from Thailand (case 5). The brains of 2 adult cases examined were reported as normal (cases 2 and 3), except for lysis of the granular cells of the cerebellar cortex in one (case 3). No significant pathology was noted in the other organs. In particular, myocarditis was absent. Postmortem viral culture or RT-PCR was done on 5 cases (cases 1-5). Viral culture of the lung for the 2 patients dying at 1 month was negative (cases 1 and 2). Viral culture of the lung for case 3 dying at day 10 was positive for H5N1. Reverse transcriptase–polymerase chain reaction was done on the lung of case 4 and 5 dying at days 10 and 17, respectively, and both were positive. Viral culture or RT-PCR was done in other organs including the brain, kidney, liver, bone marrow, heart, intestine, lymph node, and spleen. These were all negative except for one case. For case 5, RT-PCR of small and large intestine and the spleen was positive for H5N1. The relevant investigators have also demonstrated positive-stranded viral RNA indicating viral replication only in the lung and intestine [29]. Another clinical article had reported a broader occurrence of H5N1 in other organs. A 4-year-old boy in Vietnam presented with diarrhea followed by encephalopathy and death [31]. H5N1 influenza virus was isolated from the cerebrospinal fluid, rectal swab, throat, and serum specimens. This was actually the first report of isolation of H5N1 from extrapulmonary sites. Unfortunately, postmortem was not done and the pathology of the gastrointestinal tract and brain was unknown.

3.3. Comparison of the pathology of SARS and H5N1

The comparison is summarized in Table 3. The comparative features are drawn from the reviewed literature, their accompanying figure, and the authors' experience. These features have been summarized in the review sections on the

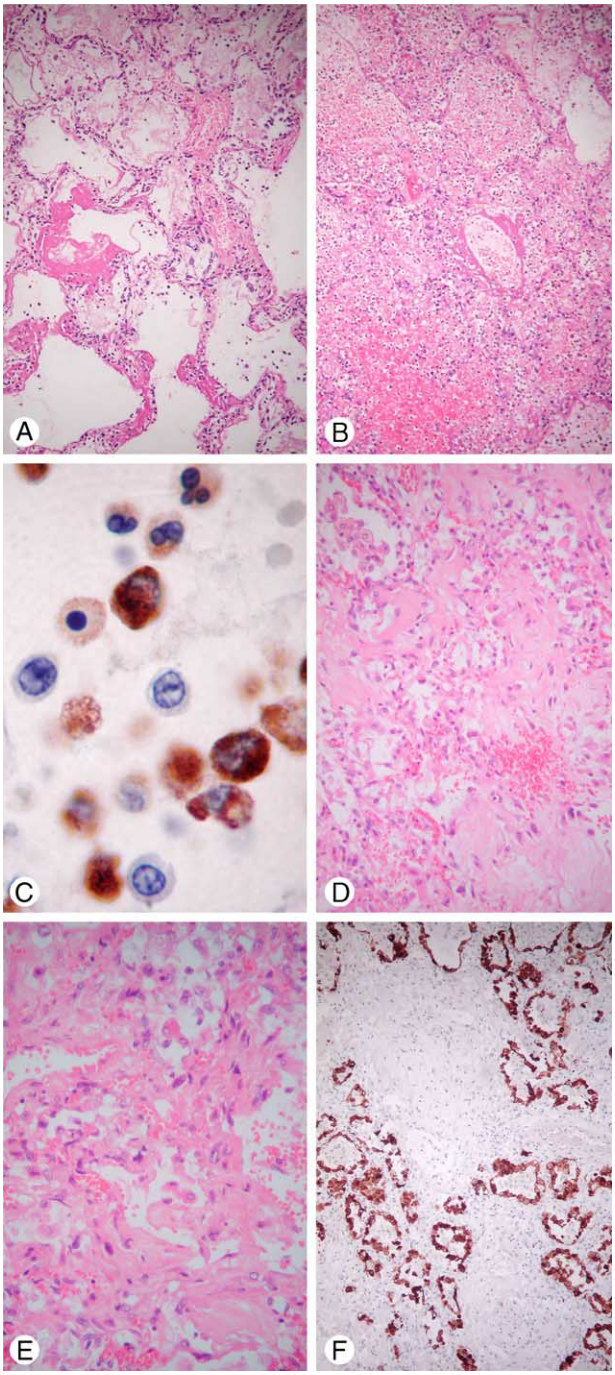

Fig. 3 Pulmonary pathology of H5N1. A, Acute exudative DAD with hyaline membrane. B, Necrotizing and hemorrhagic area of DAD. C, Mixed inflammatory cell exudates in acute DAD labeled with the histiocytic marker CD68. Note the strongly reactive histiocytic cells, weakly reactive neutrophils, and unreactive lymphocytes (D, E). Organizing DAD with interstitial hyaline and paucicellular fibrosis. F, Pneumocytic hyperplasia labeled by the epithelial marker AE1/AE3. Note area of alveolar destruction with patchy and interstitial fibrosis (hematoxylin-eosin stain unless specified, original magnification ×630 [2C], ×200 [2E], and ×100 [all others]; A-C taken from a patient with H5N1 dying on day 10 [case 3 of Table 2]; D-F taken from a patient with H5N1 dying on day 30 [case 1 of Table 2]).

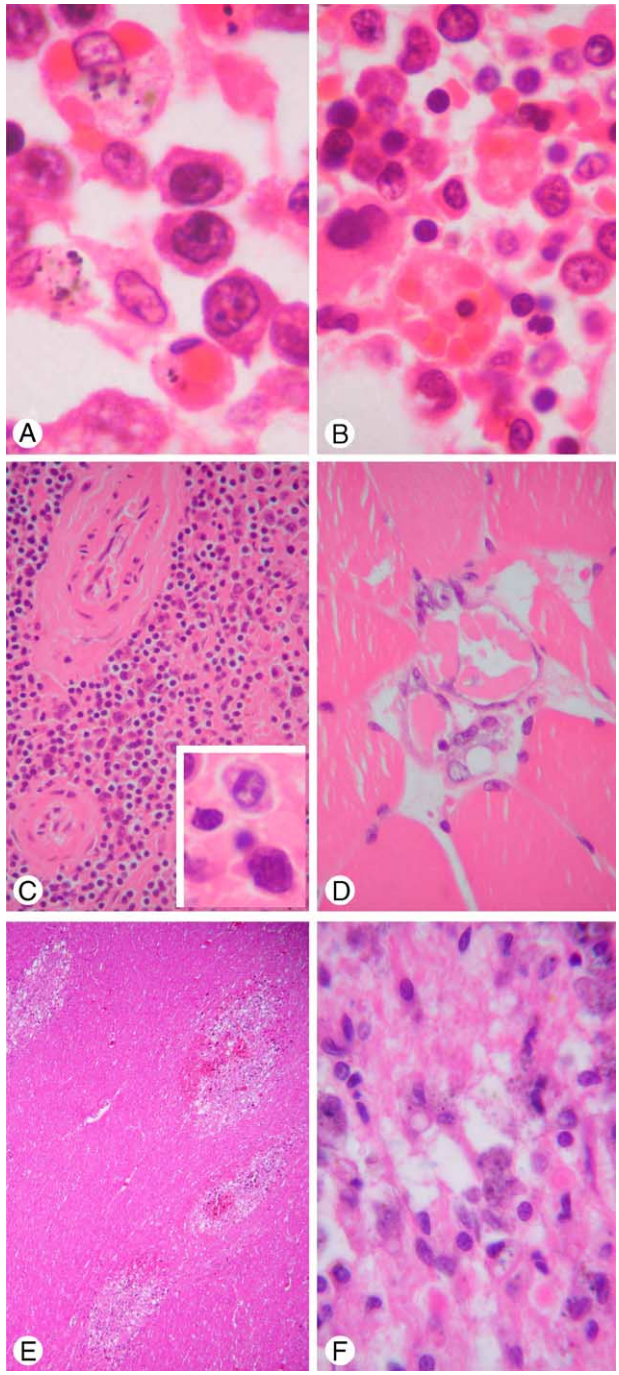

Fig. 4 Extrapulmonary pathology of H5N1. A, Reactive hemophagocytosis in pulmonary hilar lymph node and 3 large activated lymphocytes in the center of field. B, Reactive hemophagocytosis in bone marrow. C, Lymphoid depletion in spleen and large activated lymphocytes in inset. D, Skeletal muscle fiber necrosis. E, Microglial nodules with rarefaction and demyelination in cerebral white matter. F, High-power view of microglial nodule with a few axon balls in the lower field and foamy and pigment-laden macrophages (hematoxylin-eosin stain, original magnification ×1000 [A, B, and C inset], ×100 [4E], ×400 [all others]; A-D taken from a patient with H5N1 dying on day 10 [case 3 of Table 2]; E and F taken from a patient with H5N1 dying on day 30 [case 1 of Table 2]).

Table 3 Comparative pathology of SARS and H5N1

Similarities	Differences
1. Pneumocyte the primary target of infection	1. SARS: less fulminant progression of DAD with combination of acute and reparative patterns; H5N1: more fulminant progression of DAD
2. Diffuse alveolar damage	2. SARS: more fibrocellular intra-alveolar organization with BOOP-like pattern, multinucleated histiocytes, and pneumocytes in 66%; H5N1: more hemorrhagic and necrotizing alveoli in acute phase, interstitial hyaline and paucicellular fibrosis, scanty intra-alveolar organization with no BOOP-like pattern, inconspicuous multinucleated cells. (limited by inadequate data)
3. Systemic cytokine activation with reactive hemophagocytic syndrome	3. SARS-CoV: recoverable from lung by RT-PCR up to day 42; H5N1 virus: recoverable from lung by RT-PCR up to day 17
4. Lymphoid depletion in spleen	4. SARS-CoV: more widespread dissemination to blood, urine, feces, gastrointestinal tract, and liver; H5N1 virus: until recently only isolated from lung, recent report of extrapulmonary isolation from gastrointestinal tract, cerebrospinal fluid, and blood
5. Skeletal muscle fiber necrosis	5. SARS: no documented involvement of brain; H5N1: evidence of cerebral involvement in 2 autopsied cases and one clinical case
6. Acute tubular necrosis	

2 individual diseases. These are further substantiated and discussed below. There are substantial pathologic data on SARS, but that on H5N1 are very limited. Therefore, this comparison is tentative and provisional. More pathologic studies on H5N1 are required.

4. Discussion

Both SARS and H5N1 share similar pathology and pathogenesis. Pneumocytes are the primary target of the infection. The extensive pneumocyte destruction and the inflammatory and immune reaction elicited by the viruses cause diffuse alveolar damage. The activation of the cytokines is part of the immune reaction to eradicate the virus. The systemic cytokine activation results in reactive hemophagocytic syndrome in the lymphoreticular system and possibly also mediates other organ damage such as the skeletal muscle fiber necrosis. The lymphoid depletion in the spleen and lymph node in fatal cases may be due to combination of lymphoid necrosis and apoptosis and exhaustion of lymphoid proliferation in response to the cytokine overdrive. The acute tubular necrosis is likely to be the consequence of systemic hypoxia and shock rather than direct invasion of the viruses.

Compared with H5N1, SARS appears to show a less fulminant progression of the DAD. Features of acute DAD are often seen in combination with reparative phase in different parts of the lung. In contrast, H5N1 shows more fulminant and rapidly progressive DAD. This is in keeping with the clinical observations. The development of acute respiratory distress syndrome in SARS is generally in the second week of the illness (first peak on day 11) [32], whereas that for H5N1 is at the end of the first week (median time, day 6) [30]. On histology, DAD shows common pathologic features and distinction of the etiologic agent is not possible. Furthermore, there is difficulty in confirming or excluding SARS in a lung biopsy in the early stage of disease because of its focal involvement and the nonspecific changes. The demonstration of SARS-CoV by immunohistochemistry or in situ hybridization in infected cells would be helpful. The presence of atypical multinucleated pneumocytes and multinucleated histiocytes is characteristic of SARS, and these cells are inconspicuous in H5N1. However, such changes are nonspecific because other viral infection such as respiratory syncytial virus and measles may also produce giant cells. Based on the pathologic description and figures in the published reports, the organizing phase of SARS appears quite fibrocellular and intra-alveolar with a BOOP-like pattern. This may explain the empirical success of high-dose corticosteroid in SARS because BOOP is known to respond to corticosteroid. However, in one case treated by high-dose corticosteroid studied by the authors, BOOP still occurred in a lesser extent. For H5N1, the pathologic data are limited. Based on the observation by the authors, the acute DAD appears more necrotizing and hemorrhagic. The alveolar destruction causes foci of fibrosis without pneumocytic regeneration. The organizing phase is also marked by interstitial fibrosis of a hyaline and paucicellular form without BOOP-like pattern.

The SARS-CoV appears recoverable by RT-PCR in the lung for a much longer time (up to day 42) compared with H5N1 (up to day 17). The SARS-CoV appears more widely spread in the human body, including dissemination to the blood, urine, feces, gastrointestinal tract, and liver. Until recently, the extrapulmonary isolation of H5N1 had been negative. There is recent documentation of isolation of H5N1 from the gastrointestinal tract, cerebrospinal fluid, and blood [29,31]. As the virus H5N1 may undergo adaptational mutation to the new human host environment, wider pathologic targets in the human body may become possible. Biopsy and postmortem study of new human H5N1 cases are

urgently needed for further elaboration. In ducks, H5N1 is a systemic disease affecting multiple organs including the central nervous system [33]. So far, evidence of cerebral involvement is noted in 2 autopsied cases (cases 1 and 5) and 1 clinical case [31]. All these 3 cases were children aged 4 to 13 years and may indicate a predisposition in children.

One of the key issues in the management of both SARS and H5N1 is the early eradication of the virus. The long persistence of SARS-CoV in the postmortem lung tissue indicated the failure of the drugs, including ribavirin, that had been used. The persistence of H5N1 in postmortem lung is also generally longer than human influenza virus. This is probably due to the lack of crossing reacting antibodies in the human host, unlike human influenza virus subtypes. The occasional report of the resistance of H5N1 virus to oseltamivir is a cause for concern [34]. The persistence of the virus also highlights the importance of precautions against infection during postmortem examination despite death after long clinical illness. Another key issue in the management of both SARS and H5N1 is to control or downgrade the inflammatory response in the DAD. However, as pointed out by Yuen et al [35], the use of immunomodulators may be counterproductive if their use would delay the eradication of the virus.

In conclusion, both SARS and H5N1 share similar pathology and pathogenesis. H5N1 appears more fulminating and carries a mortality about 5-fold that of SARS. The management of both SARS and H5N1 would involve earliest eradication of the virus by appropriate antiviral regime and possible immunomodulation to downgrade or control the diffuse alveolar damage. The optimal ways to achieve these targets still await further exploration.

Acknowledgments

The authors thank the Virus Unit, Department of Health, Hong Kong Special Administrative Region, and the Centers for Disease Control and Prevention, Atlanta, Ga, for the microbiological confirmation of the reported cases. The manuscript was expertly prepared by Ms Irene Hui, Personal Secretary.

References

[1] WHO guidelines for the global surveillance of severe acute respiratory syndrome (SARS). Updated recommendations, October 2004. World Health Organization [online]. Available at http://www.who.int/csr/resources/publications/WHO_CDS_CSR_ARO_2004_1/en/index.html.

[2] Summary table of SARS cases by country, 1 November 2002–7 August 2003. 15 August 2003. World Health Organization [online]. Available at http://www.who.int/csr/sars/country/2003_08_15/en/index.html.

[3] Yuen KY, Chan PK, Peiris M, et al. Clinical features and rapid viral diagnosis of human disease associated with avian influenza A H5N1 virus. Lancet 1998;351:467-71.

[4] Peiris JSM, Yu WC, Leung CW, et al. Re-emergence of fatal human influenza A subtype H5N1 disease. Research letters. Lancet 2004;363:617-9.

[5] World Health Organization. Communicable disease surveillance and response. Cumulative number of confirmed human cases of avian influenza A (H5N1) reported to WHO, dated 30 December 2005 [online]. Available at http://www.who.int/csr/disease/avian_influenza/country/cases_table_2005_12_30/en/index.html.

[6] Nicholls JM, Pool LLM, Lee KC, et al. Lung pathology of fatal severe acute respiratory syndrome. Lancet 2003;361:1773-8.

[7] Tse GMK, To KF, Chan PKS, et al. Pulmonary pathological features in coronavirus associated severe acute respiratory syndrome (SARS). J Clin Pathol 2004;57:260-5.

[8] Cheung OY, Chan JWM, Ng CK, et al. The spectrum of pathological changes in severe acute respiratory syndrome (SARS). Histopathology 2004;45:119-24.

[9] Lang ZW, Zhang LJ, Zhang SJ, et al. Pathological study on severe acute respiratory syndrome. Chin Med J 2003;116:976-80.

[10] Ding YQ, Wang HJ, Shen H, et al. The clinical pathology of severe acute respiratory syndrome (SARS): a report from China. J Pathol 2003;200:282-9.

[11] Hsiao CH, Wu MZ, Chen CL, et al. Evolution of pulmonary pathology in severe acute respiratory syndrome. J Formos Med Assoc 2005;104:75-81.

[12] Franbs TJ, Chong PY, Chui P, et al. Lung pathology of severe acute respiratory syndrome (SARS): a study of 8 autopsy cases from Singapore. Hum Pathol 2003;34:743-8.

[13] Chong PY, Chui P, Ling AE, et al. Analysis of deaths during the severe acute respiratory syndrome (SARS) epidemic in Singapore. Challenges in determining a SARS diagnosis. Arch Pathol Lab Med 2004;128:195-204.

[14] Hwang DM, Chamberlain DW, Poutanen SM, et al. Pulmonary pathology of severe acute respiratory syndrome in Toronto. Mod Pathol 2005;18:1-10.

[15] Chau TN, Lee KC, Yao H, et al. SARS-associated viral hepatitis caused by a novel coronavirus: report of three cases. Hepatology 2004;39:302-10.

[16] Leung WK, To KF, Chan PK, et al. Enteric involvement of severe acute respiratory syndrome-associated coronavirus infection. Gastroenterology 2003;125:1011-7.

[17] Leung TW, Wong KS, Hui AC, et al. Myopathic changes associated with severe acute respiratory syndrome. A postmortem case series. Arch Neurol 2005;62:1113-7.

[18] Chu KH, Tsang WK, Tang CS, et al. Acute renal impairment in coronavirus-associated severe acute respiratory syndrome. Kidney Int 2005;67:698-705.

[19] Wong RSM, Wu A, To KF, et al. Haematological manifestations in patients with severe acute respiratory syndrome: retrospective analysis. BMJ 2003;326:1358-82.

[20] To KF, Tong JHM, Chan PKS, et al. Tissue and cellular tropism of the coronavirus associated with severe acute respiratory syndrome: an in-situ hybridization study of fatal cases. J Pathol 2004;202:157-63.

[21] Shieh WJ, Hsiao CH, Paddock CD, et al. Immunohistochemical, in situ hybridization and ultrastructural localization of SARS-associated coronavirus in lung of a fatal case of severe acute respiratory syndrome in Taiwan. Hum Pathol 2005;36:303-9.

[22] Ding Y, He L, Zhang Q, et al. Organ distribution of severe acute respiratory syndrome (SARS) associated coronavirus (SARS-CoV) in SARS patients: implications for pathogenesis and virus transmission pathways. J Pathol 2004;203:622-30.

[23] Choi KW, Chau TN, Tsang O, et al. Outcomes and prognostic factors in 267 patients with severe acute respiratory syndrome in Hong Kong. Ann Intern Med 2003;139:715-23.

[24] Beasley MB, Franks TJ, Galvin JR, et al. Acute fibrinous and organizing pneumonia: a histological pattern of lung injury and

possible variant of diffuse alveolar damage. Arch Pathol Lab Med 2002;126:1064-70.
[25] Lau KK, Yu WC, Chu CM, et al. Possible central nervous system infection by SARS coronavirus. Emerg Infect Dis 2004;10:342-4.
[26] To KF, Chan PKS, Chan KF, et al. Pathology of fatal human infection associated with avian influenza A H5N1 virus. J Med Virol 2001; 63:242-6.
[27] Ungchusak K, Auewarakul P, Dowell SF, et al. Probable person-to-person transmission of avian influenza A (H5N1). N Engl J Med 2005;352:333-40.
[28] Chokephaibulkit K, Uiprasertkul M, Puthavanthana P, et al. A child with avian influenza A (H5N1) infection. Pediatr Infect Dis J 2005; 24:162-6.
[29] Uiprasertkul M, Puthavathana P, Sangsiriwut K, et al. Influenza A H5N1 replication sites in humans. Emerg Infect Dis 2005;11: 1036-41.
[30] Chotpitayasunondh T, Ungchusak K, Hanshaoworakul W, et al. Human disease from influenza A (H5N1), Thailand, 2004. Emerg Infect Dis 2005;11:201-9.
[31] de Jong MD, Cam BV, Qui PT, et al. Fatal avian influenza A (H5N1) in a child presenting with diarrhea followed by coma. N Engl J Med 2005;352:686-891.
[32] Peiris JSM, Chu CM, Cheng VCC, et al. Clinical progression and viral load in a community outbreak of coronavirus-associated SARS pneumonia: a prospective study. Lancet 2003;361:1767-72.
[33] Sturm-Ramirez KM, Ellis T, Bousfield B, et al. Re-emerging H5N1 influenza viruses in Hong Kong in 2002 are highly pathogenic to ducks. J Virol 2004;78:4892-901.
[34] Maila Q, Kiso M, Someya K, et al. Isolation of drug-resistant H5N1 virus. Brief communication. Nature 2005;437:1108.
[35] Yuen KY, Wong SSY. Human infection by avian influenza A H5N1. Hong Kong Med J 2005;11:189-99.